Strong-field terahertz optical sideband generation for wavelength conversion in asymmetric double quantum wells

J.-Z. Zhang* and D. Allsopp

Department of Electronic and Electrical Engineering,

University of Bath, Bath, BA2 7AY, UK.

(Dated: November 20, 2009)

Abstract

Terahertz (THz) optical sideband generation in asymmetric double quantum wells (ADQWs) in strong THz fields is studied theoretically. Both monotonic THz-power dependence and saturation of the first-order sideband intensity can occur, depending on the near infrared (NIR) and THz photon energies. In both respects the calculated sideband intensity behaviour agrees with experimental findings [Appl. Phys. Lett. 75, 2728 (1999); Phys. Rev. B 70, 115312 (2004)]. The non-monotonic THz-power dependence and saturation of the sideband intensity are due to the excitonic Stark splitting. While the sideband saturation imposes limitations on the wavelength conversion efficiency, the simultaneous broadening of sideband resonances benefits wavelength conversion by increasing the number of NIR frequencies available for wavelength conversion.

PACS numbers: 71.35.-y, 71.70.Ej, 78.20.Jq, 78.47.jh

*Electronic address: J.Zhang2@bath.ac.uk

The generation of terahertz (THz) optical sidebands using quantum wells (QWs) has generated great interest due to its potential in ultrafast wavelength conversion for optical communications [1]. The electro-optic modulation involves a THz beam of frequency Ω (propagating in the QW plane) that mixes with a *weak* near-infrared (NIR) beam of frequency ω in *asymmetric* double QWs (ADQWs) [2–5] or biased single QWs [6], generating sideband emission at $\omega + n\Omega$, with $n = \pm 1, \pm 2, \pm 3, ...$ A detailed study [2] has found that, under *strong* THz fields the ω-dependent intensity, $I_{1\Omega}$, of the up-converted first-order sideband (i.e. n=1), displays a rich variety of resonances, and $I_{1\Omega}$ increases linearly with the THz power in a wide range of powers up to 2 kW. However, *non-monotonic* THz-power dependence and *saturation* of $I_{1\Omega}$ were later observed experimentally for biased ADQWs [3], unbiased ADQWs [4] and also biased single QWs [6]. The THz-power dependence of $I_{1\Omega}$ varies strongly with THz frequency [3]. The cause of these differences in experimental observations is unclear and the relationship between sideband intensity and the THz field strength needs to be resolved.

The sideband generation is a nonlinear parametric process [7, 8] with the initial and final electronic states being identical, and being the semiconductor ground state G at 0 K. We consider three energy levels, two exciton states X, X' of energies E_X, $E_{X'}$, and the ground state G of energy E_G (let $\hbar\omega_X = E_X - E_G$, $\hbar\omega_{X'} = E_{X'} - E_G$, and $\hbar\omega_{X'X} = E_{X'} - E_X > 0$). They constitute the simplest model system interacting with an NIR field $E_\omega = E_0 \cos\omega t$, and a THz field $E_\Omega = E_T \cos\Omega t$ ($\Omega \sim \omega_{X'X}$). E_Ω couples X, X', while the NIR probe induces optical polarization between G and the exciton states. The 1Ω sideband generation can be described in terms of a second-order nonlinear susceptibility $\chi^{(2)}(\omega + \Omega)$. When the THz field is weak, the $\chi^{(2)}(\omega + \Omega)$ expression has a familiar form [7]. For the $GXX'G$ parametric process shown in Fig. 1(a), $\chi^{(2)}(\omega + \Omega)$ is given by

$$\chi^{(2)}(\omega + \Omega) = \frac{2}{V\hbar^2} \frac{\langle G|\mu|X'\rangle\langle X'|\nu|X\rangle\langle X|\mu|G\rangle}{(\omega + \Omega - \omega_{X'} + i\gamma)(\omega - \omega_X + i\gamma)} , \tag{1}$$

in the rotating wave approximation (RWA) [9] with respect to the NIR field. Here μ (ν) is the projection of the dipole moment operator along the NIR (THz) field, γ is the damping rate, and V the QW volume. Exchanging $X \leftrightarrow X'$ in Eq. (1) gives $\chi^{(2)}(\omega + \Omega)$ for the $GX'XG$ process. Four resonances of $\chi^{(2)}(\omega + \Omega)$ then occur at $\omega = \omega_X, \omega_{X'}, \omega_X - \Omega, \omega_{X'} - \Omega$, with the latter two corresponding to virtual levels [Fig. 1(a), dashed lines]. The double resonance occurs where the first and fourth resonances coincide making $\chi^{(2)}(\omega + \Omega)$ reach its maximum

magnitude. Under stronger THz fields, the expressions for $\chi^{(2)}(\omega+\Omega)$ can be derived using density matrix formalism. For the $GXX'G$ process $\chi^{(2)}(\omega+\Omega)$ can be given by

$$\chi^{(2)}(\omega+\Omega)=\frac{2}{V\hbar^2\mathcal{D}_X}\langle G|\mu|X'\rangle\langle X'|\nu|X\rangle\langle X|\mu|G\rangle \ , \tag{2}$$

where $\mathcal{D}_X=(\omega-\omega_X+i\gamma)(\omega+\Omega-\omega_{X'}+i\gamma)-\Omega_R^2$, with $\Omega_R=\frac{1}{2}|\langle X'|\nu|X\rangle|E_T/\hbar$ being the Rabi frequency [9] to characterize the THz field-exciton interaction. Now $\mathrm{Re}\mathcal{D}_X=0$ yields a pair of resonances, $\omega=\omega_X+\frac{1}{2}(-\delta\pm\Delta)$, where $\delta=\Omega-\omega_{X'X}$ is the detuning of the THz field, and $\Delta=[\delta^2+4(\gamma^2+\Omega_R^2)]^{\frac{1}{2}}$ is the frequency separation between the pair. The pair correspond to the two split levels of E_X. The $\chi^{(2)}(\omega+\Omega)$ expression for the $GX'XG$ process yields additional two pairs of resonances, corresponding respectively to the splittings of levels $E_{X'}$ and $E_X-\hbar\Omega$ (Fig. 1). All these pairs of levels occur due to the optical Stark effect (OSE) [hence the level splittings are Stark splittings (SSs)] [10]. In the weak THz field regime, $\Omega_R\ll\gamma$, Eq. (2) simply reduces to Eq. (1).

Eq. (1) has been applied to explain the observed double-resonance sideband emission [4–6, 11]. However it cannot explain the detailed features in the sideband resonance spectrum ($I_{1\Omega}$ vs $\hbar\omega$). The experimentally observed saturation behaviour [4, 6] clearly demands an equation beyond Eq. (1). In this letter, we report on the sideband generation in ADQWs in strong THz fields, based on the calculation of the optical polarization with a microscopic model. Our calculated sideband resonance spectra and THz-power dependences of sideband intensities are in good agreement with experimental results. They can be well explained using Eq. (2).

The following calculation is based on a two-band semiconductor model. The electron and hole are treated as single particles within the effective mass theory. Let en and hl denote the electron subband of index n and the hole subband of index l, respectively. The ADQW interacts with a *weak* NIR field E_ω and a THz field E_Ω simultaneously. Sideband emission occurs due to the induced interband polarization $P(t)$. The equation of motion for the polarization components $p_{ln\mathbf{k}}$ can be written as [12]

$$\frac{\partial p_{ln\mathbf{k}}}{\partial t}=\frac{i}{\hbar}\Bigg[-(E^e_{n\mathbf{k}}+E^h_{l\mathbf{k}})\ p_{ln\mathbf{k}}+\mu_{nl\mathbf{k}}E_\omega+\sum_{l',n',\mathbf{k}'}V_{nn'l'l}(|\mathbf{k}-\mathbf{k}'|)p_{l'n'\mathbf{k}'}$$

$$+E_\Omega\left(\sum_{n'}\xi_{nn'}p_{ln'\mathbf{k}}+\sum_{l'}\zeta_{l'l}p_{l'n\mathbf{k}}\right)\Bigg]-\gamma_p p_{ln\mathbf{k}} \ . \tag{3}$$

$E^e_{n\mathbf{k}}$ and $E^h_{l\mathbf{k}}$ are the electron and hole subband energies ($\mathbf{k}$ is the two-dimensional wavevector). $\mu_{nl\mathbf{k}}$ is the interband dipole matrix element, and $\xi_{nn'}$ ($\zeta_{l'l}$) is the intersubband dipole matrix element connecting two electron (hole) subbands n, n' (l', l). $V_{nn'l'l}(q)$ is the QW interband Coulomb matrix elements commonly used in the literature [13], with q being the modulus of the transfer wavevector $\mathbf{q} = \mathbf{k} - \mathbf{k}'$. γ_p is the polarization dephasing rate. Let X_{enhl} denote the $en - hl$ exciton having energy $E_{enhl} = \hbar\omega_{enhl}$. Coulombic coupling (CC) between excitons X_{enhl} and $X_{en'hl'}$ [14] occurs when nonzero Coulomb matrix elements $V_{nn'l'l}(q)$ and $V_{n'nll'}(q)$ exist.

The coupled polarization equations [Eq. (3)] are numerically solved to give solutions $p_{ln\mathbf{k}}(t)$. The singularity of the Coulomb potential is treated by adopting the modified quadrature technique [13]. Knowing $p_{ln\mathbf{k}}(t)$, the interband polarization $P(t)$ is then calculated from $P(t) = \frac{1}{V}\sum_{n,l,\mathbf{k}} p_{ln\mathbf{k}}\mu^*_{nl\mathbf{k}} + c.c.$. Let $E(\pm\omega)$ and $E(\pm\Omega)$ be the Fourier components of the light fields [7]. In the RWA [9], $P(t)$ can be expanded as $P(t) = \epsilon_b\chi^{(1)}(\omega)E(\omega) + \epsilon_b\chi^{(2)}(\omega\pm\Omega)E(\omega)E(\pm\Omega) + \epsilon_b\chi^{(3)}(\omega\pm 2\Omega)E(\omega)E(\pm\Omega)E(\pm\Omega) + ...$, to give the linear susceptibility $\chi^{(1)}(\omega)$ and the nonlinear susceptibilities of various orders $\chi^{(2)}(\omega \pm \Omega)$, $\chi^{(3)}(\omega \pm 2\Omega)$, ...

The ADQW structure investigated here consists of 75 $\mathring{A}$ and 85 $\mathring{A}$ GaAs wells separated by a 23 $\mathring{A}$ $Al_{0.3}Ga_{0.7}As$ middle barrier while embedded in two outer $Al_{0.3}Ga_{0.7}As$ barriers, the same as that of the sample in experiment [2]. The *in-plane* polarized continuous-wave NIR probe in experiments is modeled as a Gaussian pulse of 8 ps full width at half maximum irradiance, with a variable centre frequency. The material parameters are taken from Ref. [15]. The dephasing rate γ_p=1.52 THz corresponds to the energy broadening of 2 meV in experiments [2, 6]. Calculations are performed using two electron subbands and four heavy-hole subbands.

Figure 2(a) shows the 1Ω sideband intensity versus $\hbar\omega$ for a THz field of f=2.5 THz and intensity I_{THz}=1.5 MW/cm^2. This result is in good agreement with the experimental data [2] [compare to Fig. 4(b) of Ref. [2], f=2.5 THz, I_{THz}=2 MW/cm^2]. According to our three-level model [Eq. (2)], any two excitons that couple via the THz field may contribute to the sideband generation. To identify the peaks in Fig. 2(a), we need to separate the contributions to the sideband generation from the 16 pairs of excitonic levels. Our calculation indicates that large contributions are made from the two pairs (X_{e1h1}, X_{e2h1}) and (X_{e1h2}, X_{e2h2}) [Fig. 2(b)]. Exact resonance with X_{e1h2} and X_{e2h2} occurs for f=2 THz fields. The f=2.5

THz field is 2 meV off resonance. A strong peak at 1.5675 eV, with a lower-energy shoulder at 1.5646 eV, dominates the sideband intensity spectrum of the (X_{e1h2}, X_{e2h2}) pair. They correspond to the two resonances of $\chi^{(2)}(\omega+\Omega)$ due to the splitting of X_{e1h2}. The peak at 1.5577 eV and the small feature at 1.5534 eV are the two resonances due to the splitting of the virtual level $E_{e1h2}-\hbar\Omega$. In the energy range of X_{e2h2} splitting of X_{e2h2} does not occur; instead a broad feature exists. In fact, there is strong CC between excitons X_{e1h2} and X_{e2h2}, which has caused significant changes to the sideband resonance spectrum. For example, when the CC is not taken into account, three pairs of features corresponding to the splittings of $E_{e1h2}-\hbar\Omega$, E_{e1h2} and E_{e2h2} are clearly resolved in the calculated spectrum. The sideband intensities are significantly enhanced when taking the CC into account. Similar 1Ω sideband peak splitting was also observed in another experiment [6] [Fig. 6(a) of Ref. [6]].

We calculated the dependence of the sideband intensity on I_{THz} for both the first- and second-order sidebands at various THz and NIR photon energies. Fig. 3(a) shows the results of the 1Ω and 2Ω sidebands, at f=2.5 THz for NIR excitation at the energy of X_{e1h1} (1.562 eV), as is the case in experiment [2]. The intensities of both sidebands increase monotonically with the THz intensity. The 1Ω sideband shows approximately a linear I_{THz} dependence while the 2Ω sideband displays a quadratic dependence. Both dependences have been observed in experiment [2].

$I_{1\Omega}$ does not always increase monotonically with the THz power. As shown in Fig. 3(b) where $\hbar\omega$ sits at the X_{e1h2} energy, the 1Ω sideband emission reaches a maximum at 1.5 MW/cm^2 and then slightly decreases with further increasing I_{THz}. Indeed, recent experiments [3, 4, 6] have found that $I_{1\Omega}$ saturates at high THz powers. This can be explained again using Eq. (2). The f=2.5 THz fields are near resonance with X_{e1h2} and X_{e2h2}. For NIR excitation with $\omega\sim\omega_{e1h2}$, the 1Ω sideband emission is governed by the $GX_{e1h2}X_{e2h2}G$ process [refer to Fig. 2(b)]. $I_{1\Omega}\propto|\chi^{(2)}(\omega+\Omega)|^2 I_{THz}$. In a strong THz field Re$\mathcal{D}_X$ in the denominator of $\chi^{(2)}(\omega+\Omega)$ [Eq. (2)] can be approximately given by $\mathcal{D}_X\approx(\omega-\omega_{e1h2}-\Omega_R)(\omega-\omega_{e1h2}+\Omega_R)$. The contribution from the Rabi frequency Ω_R becomes increasingly important causing $I_{1\Omega}$ to deviate from the simple linear dependence on I_{THz}. Mathematically, the denominator of $|\chi^{(2)}(\omega+\Omega)|^2$ contains $\Omega_R^4\propto I_{THz}^2$, making $|\chi^{(2)}(\omega+\Omega)|^2$ decrease fast at high THz intensities. Physically, both the levels of X_{e1h2} and X_{e2h2} split due to the OSE, causing broadening to the $\chi^{(2)}(\omega+\Omega)$ resonance spectrum while *reduction* in its spectral intensities. Therefore,

$I_{1\Omega}$ decreases rather than increases as I_{THz} further increases.

In contrast, the $I_{1\Omega}$ in Fig. 3(a) does not show significant deviation from the linear dependence. This is because the f=2.5 THz fields are far off resonance with X_{e1h1} and X_{e2h1}. When the *resonant* THz fields of f=3.8 THz are used, the resulting $I_{1\Omega}$ does saturate [Fig. 3(a), dotted line] due to the SSs of X_{e1h1} and X_{e2h1}.

The experimentally observed saturation of $I_{1\Omega}$ was attributed to broadening of the sideband resonance [6]. Three possible causes for the broadening were pointed out [6]: (i) the excitonic level splitting, (ii) lattice heating, and (iii) deviation of $\mathbf{E}_\Omega$ from the growth-direction. Our study has verified that, significant excitonic SSs do cause power saturation to $I_{1\Omega}$, even when the other two factors are absent.

Strong sideband emission is key to high wavelength conversion efficiencies. Our study indicates that, to seek large sideband intensity for efficient wavelength conversion, the THz field should be properly strong. Too intense THz fields ($\Omega_R \gg \gamma$) will instead reduce the peak intensity and hence the conversion efficiency. On the other hand, a broadened sideband resonance spectrum is also useful for wavelength conversion [1], as it provides a range of tunable NIR frequencies rather than a few limited frequencies only. More interestingly, such spectral broadening is realized by the excitonic SS. The broadening can be tuned simply by altering the THz field strength.

In conclusion, we studied THz optical sideband generation in ADQWs under strong THz fields. Our calculated sideband resonance spectra and dependences of sideband intensities on THz power are in good agreement with experimental results. The non-monotonic THz-power dependence and saturation of the first-order sideband intensity are due to the excitonic SS. These results can be well explained using a transparent expression for the second-order nonlinear susceptibility. The sideband saturation imposes limitations on the wavelength conversion efficiency. However, simultaneous broadening of sideband resonances is beneficial to wavelength conversion, with a broad band of NIR frequencies being made available for wavelength conversion.

The authors thank Chris Phillips, Imperial College, for helpful discussions. This research was funded by the EPSRC under grant EP/D502241/1 "PORTRAIT".

[1] H. J. R. Dutton, *Understanding Optical Communications* (Prentice Hall, New Jersey, 1998).

[2] C. Phillips, M. Y. Su, M. S. Sherwin, J. Ko, and L. Coldren, Appl. Phys. Lett. **75**, 2728 (1999).

[3] M. Y. Su, S. G. Carter, M. S. Sherwin, A. Huntington, and L. A. Coldren, Phys. Rev. B **67**, 125307 (2003).

[4] S. G. Carter, V. Ciulin, M. S. Sherwin, M. Hanson, A. Huntington, L. A. Coldren, and A. C. Gossard, Appl. Phys. Lett. **84**, 840 (2004).

[5] S. G. Carter, V. Ciulin, M. Hanson, A. S. Huntington, C. S. Wang, A. C. Gossard, L. A. Coldren, and M. S. Sherwin, Phys. Rev. B **72**, 155309 (2005).

[6] V. Ciulin, S. G. Carter, M. S. Sherwin, A. Huntington, and L. A. Coldren, Phys. Rev. B **70**, 115312 (2004).

[7] Y. R. Shen, *The Principles of Nonlinear Optics* (Wiley, New York, 1984).

[8] J. Kono, M. Y. Su, T. Inoshita, T. Noda, M. S. Sherwin, S. J. Allen, , and H. Sakaki, Phys. Rev. Lett. **79**, 1758 (1997).

[9] L. Allen and J. H. Eberly, *Optical Resonance and Two-Level Atoms* (Wiley, New York, 1975).

[10] S. H. Autler and C. H. Townes, Phys. Rev. **100**, 703 (1955).

[11] M. Y. Su, S. G. Carter, M. S. Sherwin, A. Huntington, and L. A. Coldren, Appl. Phys. Lett. **81**, 1564 (2002).

[12] A. V. Maslov and D. S. Citrin, Phys. Rev. B **62**, 16686 (2000).

[13] S.-L. Chuang, S. Schmitt-Rink, D. A. B. Miller, and D. S. Chemla, Phys. Rev. B **43**, 1500 (1991).

[14] D. K. Kim and D. S. Citrin, Phys. Rev. B **76**, 125305 (2007).

[15] I. Vurgaftman, J. R. Meyer, and L. R. Ram-Mohan, J. Appl. Phys. **89**, 5815 (2001).

FIG. 1: Diagram of the energy levels responsible for the 1Ω sideband generation in a three-level model system (see text) in (a) a weak THz field, and (b) a strong THz field. In (a) the solid (dashed) lines represent real (virtual) levels. Nonlinear NIR and THz photon processes for the strongest 1Ω sideband generation are illustrated.

FIG. 2: 1Ω sideband intensity versus NIR photon energy in the ADQW under a THz field of f=2.5 THz and intensity 1.5 MW/cm^2, calculated with electron subbands $e1$, $e2$ and hole subbands (a) $h1$, $h2$, $h3$, $h4$, (b) $h1$ (dotted) or $h2$ (dashed). In (b) the resonances are labeled in terms of the excitonic SSs, and the $I_{1\Omega}$ values on the high energy tail (dashed line) are enlarged by 20 times for clarity.

FIG. 3: Up-converted first-order (solid) and second-order (dashed) sideband intensities versus THz field intensity in the ADQW in a THz field of f=2.5 THz, for the NIR photon energy at the energy of exciton (a) X_{e1h1} (1.562 eV), and (b) X_{e1h2} (1.568 eV). In (a) the dotted line shows the result of the 1Ω sideband for THz fields of a *higher* frequency f=3.8 THz.

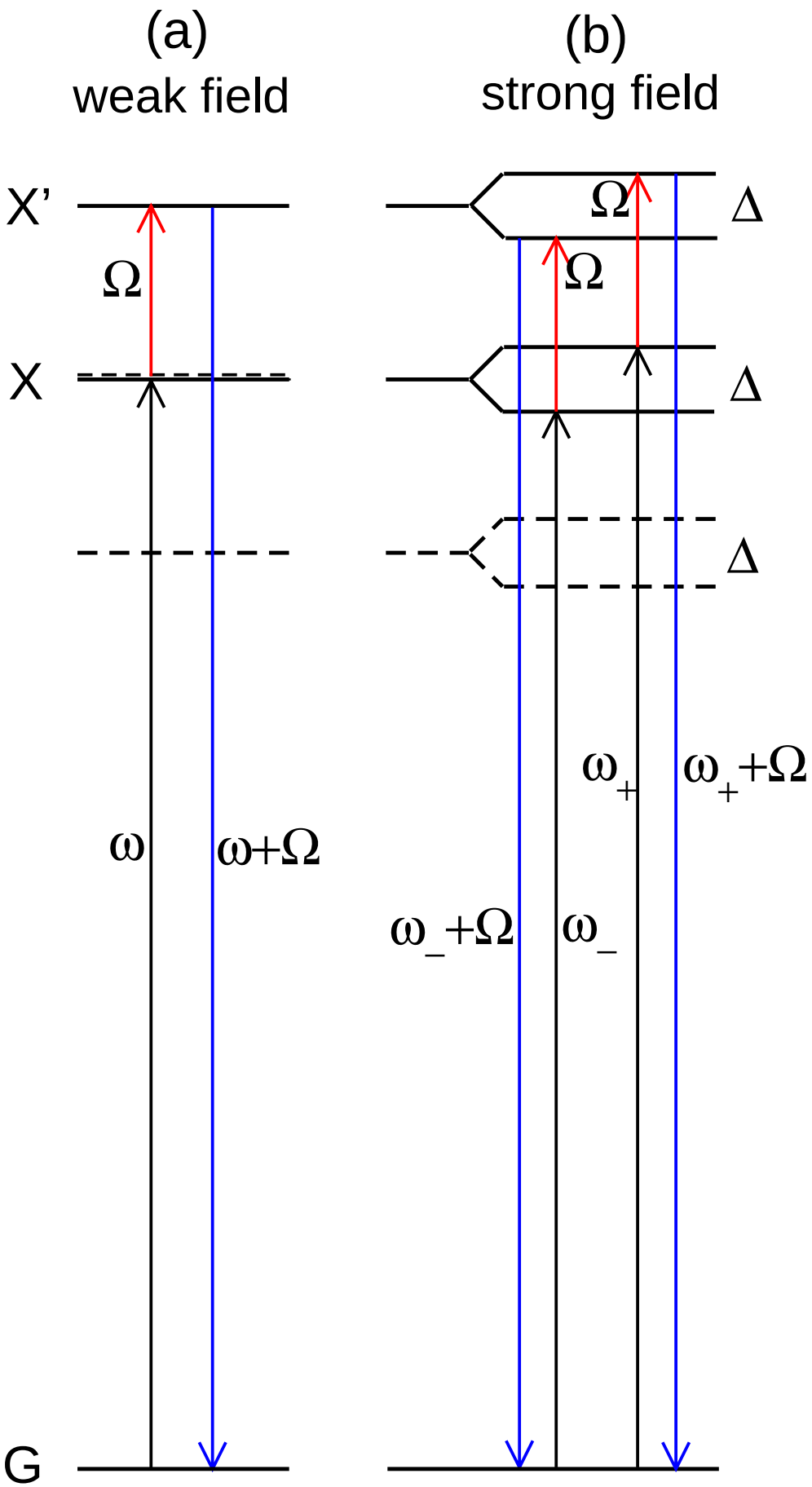
(a)
weak field
(b)
strong field
X'
X
G
Ω
ω
ω+Ω
Ω
Ω
Δ
Δ
Δ
ω+
ω++Ω
ω−+Ω
ω−

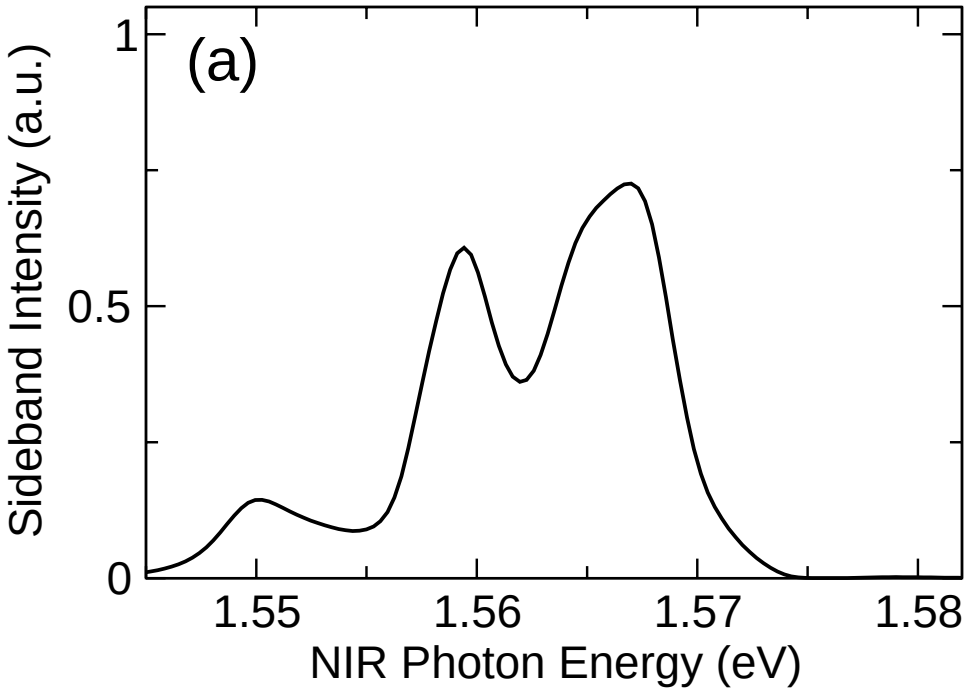
(a)
Sideband Intensity (a.u.)
1
0.5
0
1.55
1.56
1.57
1.58
NIR Photon Energy (eV)

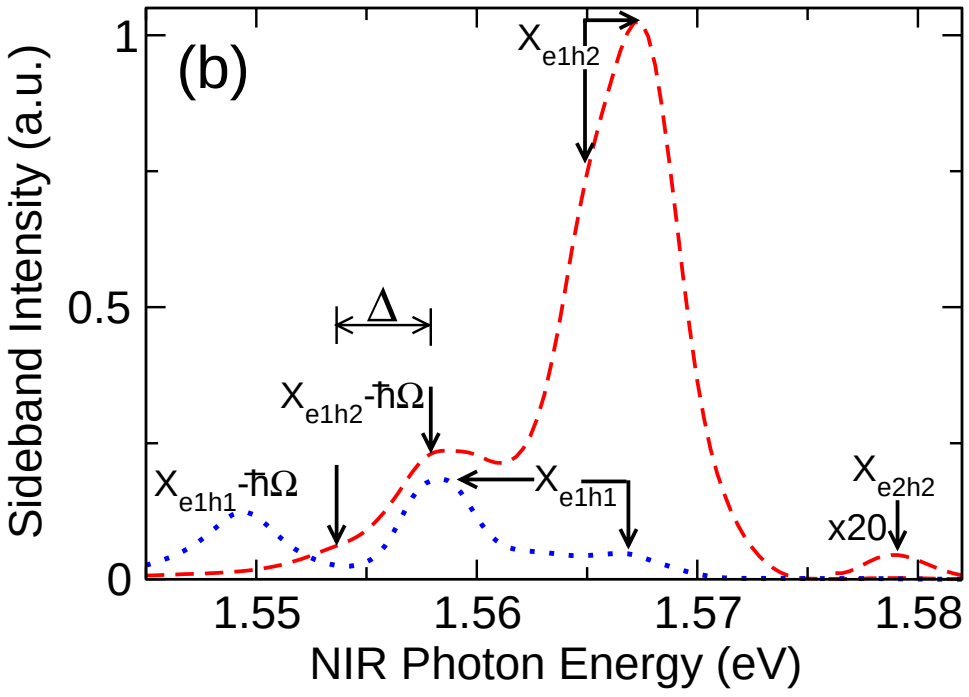
(b)
Sideband Intensity (a.u.)
1
0.5
0
X e1h2
Δ
X e1h2 -ħΩ
X e1h1 -ħΩ
X e1h1
X e2h2
x20
1.55
1.56
1.57
1.58
NIR Photon Energy (eV)

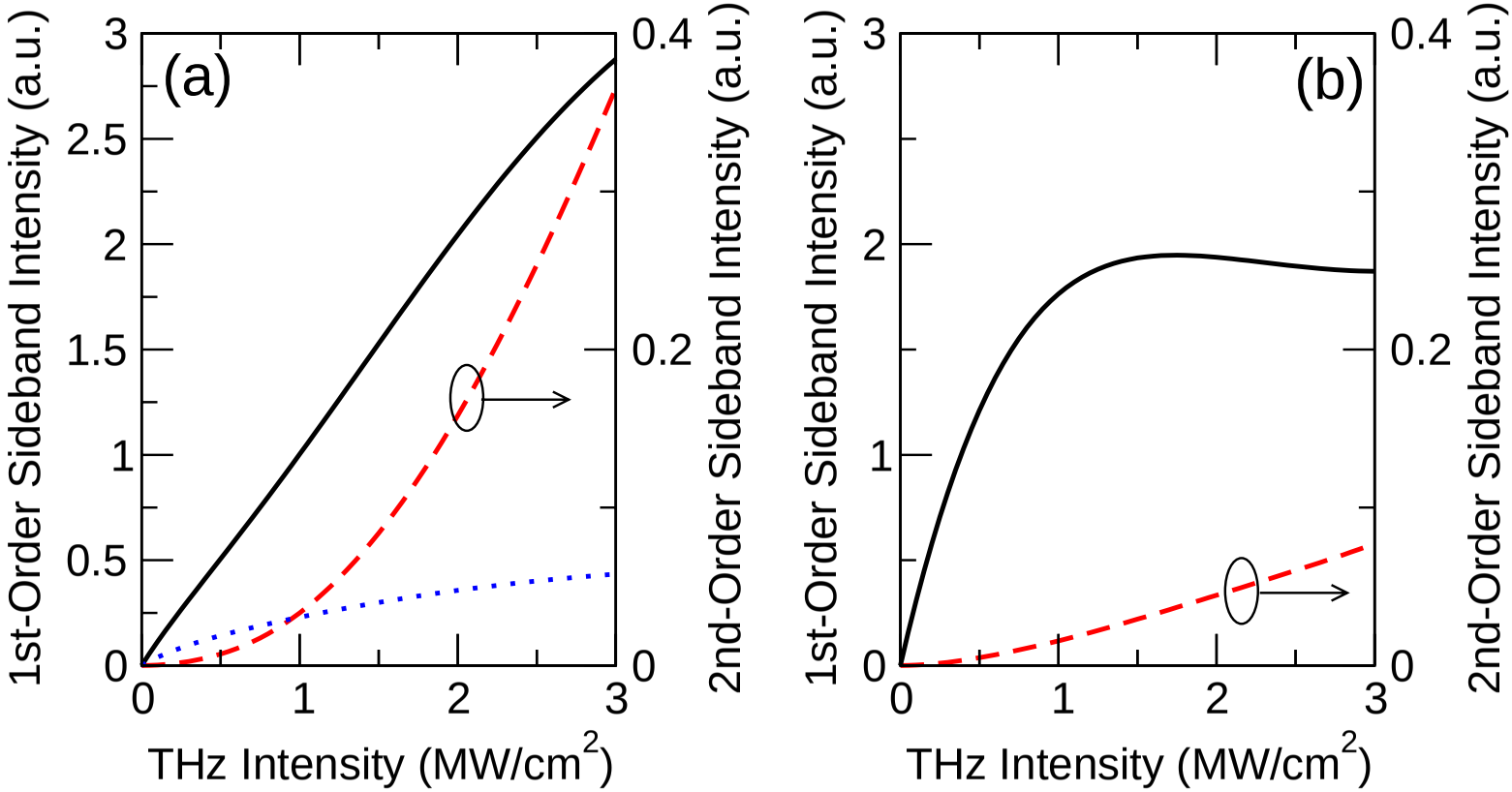
(a)
(b)
1st-Order Sideband Intensity (a.u.)
2nd-Order Sideband Intensity (a.u.)
THz Intensity (MW/cm^2)
0
0.5
1
1.5
2
2.5
3
0.2
0.4